Environ Earth Sci (2016) 75:214
DOI 10.1007/s12665-015-5060-9

ORIGINAL ARTICLE

Hydrochemical investigation of shallow groundwater in northwest margin of Lop Nur, northwest China

Zhenhua Zhao[1] · Jichun Wu[1] · Gexin Yuan[1] · Jianjie Chen[1] · Xiaofeng Xu[1] · Changhong Yan[1] · Youliang Bai[1]

Received: 3 March 2015 / Accepted: 9 September 2015 / Published online: 25 January 2016

Abstract A hydrochemical investigation was conducted in northwest margin of Lop Nur to evaluate the groundwater chemical patterns and the main hydrological processes occurring in the groundwater system. Fourteen representative groundwater samples were collected from different springs and boreholes. Hydrochemical data of the groundwater showed that SO_4, Cl-Na and Cl, SO_4-Na water types were dominant in this area, and the total dissolved solid (TDS) content rose along the flow path of the groundwater. Ionic relation analysis was used in conjunction with geochemical modeling to investigate the evolution of the chemical composition of groundwater. PHREEQC was used for inverse geochemical modeling. It is demonstrated that the groundwater, recharged mainly in the northern low mountains, acquired its mineralization properties principally from water–rock interactions, i.e., dissolution of evaporates and reverse cation exchange. The dissolution of halite, Glauber's salt, dolomite and calcite determined the Na^+, Cl^-, Mg^{2+}, Ca^{2+}, SO_4^{2-} and HCO_3^- chemistry, but evaporation and precipitation also influenced the water composition. The shallow groundwater of Lop Nur was characterized by high salinity and slow circulation.

Keywords Lop Nur · Hydrochemistry · Ionic relation · Cation exchange · Saturation index · Geochemical modeling

✉ Zhenhua Zhao
starzzh@163.com

[1] School of Earth Sciences and Engineering, Nanjing University, Nanjing 210023, China

Introduction

Lop Nur, located in the northeast of Tarim basin in China's Xinjiang Province, is one of the driest regions in the world. It is an unpopulated region characterized by low and irregular rainfall, substantial temperature variability, and high evaporation. Lop Nur has long been considered as a mysterious place, and it has unique significance from the perspectives of science, resource development, and environmental protection. Therefore, many researchers have performed continuous exploration and study from around the world since the mid-nineteenth century (Xia et al. 2007). Most research has focused on the environmental evolution of Lop Nur, the ancient Loulan Civilization, and the depression's helical salt crust structure and potash deposits (Dong et al. 2012). Great progress has been made in several aspects of understanding the region; for example, most researchers accept that plate tectonics is the most important factor for the formation of Lop Nur (Wang et al. 2001; Xia et al. 2007), and studies of the environmental evolution of Lop Nur have been conducted at different time scales, such as the Quaternary, Pleistocene, and Holocene epochs and during the historical period (Yan et al. 1998; Luo et al. 2008a, b; Wang et al. 2008; Song 2009; Zhu et al. 2009; Chang et al. 2012; Yang et al. 2013); however, the date when the lake became dry remains hotly debated (Zhong et al. 2005, 2008; Zhao et al. 2006; Li et al. 2008; Duan et al. 2013). Additionally, a huge potash reserve was discovered in the Luobei Hollow of the Lop Nur in 1995, and ever since, intensive investigations have been conducted to determine the characteristics, origins, resource abundance, and metallogenic origins of the potash deposits (Liu et al. 1999, 2002, 2003a, b, 2009, 2010; Wang et al. 2001; Jiao et al. 2003a, b, 2004, 2005; Xia et al. 2007; Zhao et al. 2014).

However, there have been few studies on groundwater systems of Lop Nur, and in particular, there has been only

one published paper on the hydrogeochemistry of Lop Nur thus far (Ma et al. 2010). It is known that Lop Nur is a large groundwater discharge playa and is also the terminal point of the Tarim Basin drainage system. Therefore, it is quite meaningful to conduct hydrological investigations for understanding the evolution of the Lop Nur groundwater system, the most difficult part of which is to collect the groundwater samples because of the harsh environment and remote location, which limit the access to researchers. This study is focused on the hydrochemical characteristics of shallow groundwater and mechanisms of water–rock interactions in northwest margin of Lop Nur. In this paper, hydrochemical techniques, as effective tools for solving various problems in hydrogeology, in arid and semi-arid regions in particular (Edmunds 2003; Al-Charideh 2012; Demiroglu et al. 2011; Han et al. 2011; Rouabhia et al. 2011; Zhu et al. 2011), were used to determine the chemical composition of groundwater and analyze the main hydrological processes controlling the groundwater chemical composition. The hydrological data and primary results in this study could be useful for researchers in studying the Lop Nur groundwater system further as well as providing a significant basis for guiding decision-making in mineral exploration of the Lop Nur region.

Geological and hydrogeological setting

The study area is located at the northwest margin of Lop Nur, between Kuruktag to the north and Konche River to the south. The area is low-lying from north to south, with a northwest to southeast tilt (Fig. 1). The altitude ranges between 900 and 2100 m above sea level. From north to south, landforms include low mountains, denuded hills, an inclined plain and an alluvial lacustrine plain. The climate is classified as temperate continental arid, with an annual precipitation of only 20–60 mm, most of which occurs in <20 days, mainly concentrated in the summer. Temporary surface floods are commonly formed after occasional storms, but the annual average evaporation capacity is up to 2900 mm. Therefore, water resources are lacking, and there are no permanent residents. The annual average relative humidity is 28.4 %. The daily maximum temperature and daily minimum temperature are 44 and −24.6 °C, respectively.

Tectonically, the study area is part of the Tarim block, and Xingdi fault is the dominant fault in the region (Xiao et al. 2010). In the low mountains area, the outcropped strata consist of igneous rock, metamorphic rock, and dolomite interbedded with tuff, sandstone, siliceous rock of Sinian and Cambrian age. In the denuded hill area and the inclined plain, the outcropped strata consist of micritic limestone interbedded with thin silty mudstone and greyish-green arkosic greywacke interbedded with bioclastic limestone of Ordovician, Silurian and Carboniferous age, and covered with a Quaternary sand layer on the southern edge of the piedmont inclined plain. In the alluvial lacustrine plain, the outcropped strata consist of Quaternary loam, sand and sandy gravel.

There is no perennial surface runoff, and all valleys are seasonal ravines, which only have temporal floods flowing after rainstorms toward southeast lowland and the Lop Nur dry lake (Fig. 1). Several springs are distributed around the

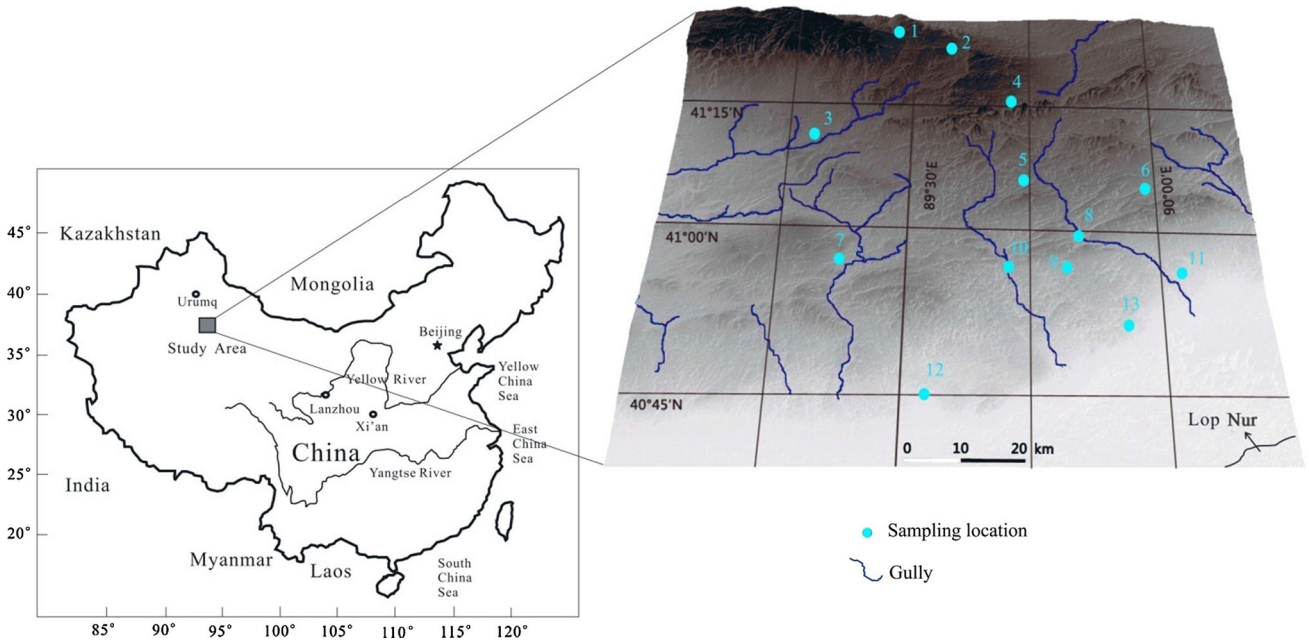

Fig. 1 Map of the study area and groundwater sampling locations

tectonic zone; evaporation occurs rapidly. Groundwater recharge mainly depends on the infiltration of atmospheric precipitation in the northern low mountains, and the groundwater discharge is dominated by evaporation while flowing from northwest to southeast. Through geophysical exploration, it was believed that there were two aquifers. Because the depth of lower aquifer is over 150 m and there are only several shallow boreholes (approximately 100 m), the emphasis of this study was concerned only with the upper aquifer. The upper aquifer is unconfined, with water-bearing media of Silurian sandstone and limestone in the bedrock area and sand or sandy gravel in the southern alluvial plain. The depth of the shallow groundwater shows a decline from north to south, at approximately 60 m in the piedmont, 20–40 m in the inclined plain, and 10–15 m in the alluvial lacustrine plain.

Sampling and analytical methods

Sampling

Because of the remote location and harsh natural environment, precious hydrological investigation of the study area is inadequate, with sparse boreholes and no residential wells; therefore, it is very difficult to collect more groundwater samples. In this study, 14 shallow groundwater samples were collected (location marked in Fig. 1). Among them, No. 1, No. 2, No. 4, No. 7, No. 8, No. 10 and No. 13 were collected from springs, and the rest of the samples were collected from boreholes. Sampling depth was 27–60 m. The boreholes were purged for 15 min before sampling. The springs were sampled directly at the outflow. Samples were subsequently filtered through 0.45-μm membranes and collected in acid-washed, well-rinsed low-density polyethylene bottles. The geographical location of all sampling sites was recorded using a GARMIN handheld global positioning system (GPS).

Alkalinity and physical parameters such as electrical conductivity (EC), pH and temperature were measured in the field using HACH portable equipment. Chemical analyses were measured at the Xinjiang Institute of Geology and Mineral Resources in Urumqi. The major ions of Na^+, K^+, Mg^{2+}, Ca^{2+}, SO_4^{2-}, Cl^-, and silica were analyzed with an Atomic Absorption Spectrometer (WFX-110) and the titration method.

Geochemical modeling

Geochemical modeling is a powerful technique for characterizing geochemical phenomena. Many programs have been developed to perform a wide variety of aqueous geochemical calculations. PHREEQC, designed by the USGS, is one of the most popular software for simulating chemical reactions and transport processes of natural or contaminated water, which has capabilities for speciation, batch-reaction, saturation index calculation, 1D reactive-transport, and inverse modeling (Parkhurst and Appelo 1999). In this study, PHREEQC 2.14.2 is used to calculate the saturation index and chemical mass transfer that has occurred during the interaction between the groundwater and rocks.

Results and discussion

Hydrochemical characteristics of groundwater

The analytical results of the groundwater samples are shown in Table 1. The groundwater samples have pH

Table 1 Geochemical data of groundwater samples in the study area

Site no.	pH	K^+ (meq/L)	Na^+ (meq/L)	Ca^{2+} (meq/L)	Mg^{2+} (meq/L)	Cl^- (meq/L)	SO_4^{2-} (meq/L)	HCO_3^- (meq/L)	H_2SiO_3 (mg/L)	TDS (mg/L)
1	6.77	0.16	11.39	5.32	5.42	7.04	11.26	4.07	10.8	1382
2	7.27	0.17	8.13	4.34	4.10	5.48	7.68	4.00	13.9	1004
3	7.2	0.11	17.46	5.26	3.83	10.14	12.10	4.68	14.0	1696
4	7.02	0.12	18.43	5.45	4.02	10.81	12.65	4.70	14.5	1704
5	7.5	0.90	41.13	7.85	3.95	22.80	22.80	3.70	10.66	3224
6	7.62	0.84	36.20	6.20	5.40	27.00	13.60	5.50	10.09	2877
7	7.7	0.98	97.26	19.51	17.92	73.49	54.65	8.77	14.37	8424
8	7.9	1.05	56.71	4.00	5.40	33.00	13.40	21.90	19.80	4022
9	7.5	1.60	135.20	24.00	22.00	87.99	86.00	12.80	22.30	11,584
10	7.79	1.11	142.80	20.76	15.97	109.30	67.92	4.15	14.6	11,196
11	7.77	2.02	288.70	30.00	25.00	215.00	125.00	4.60	15.20	21,455
12	7.75	4.26	251.10	44.00	39.99	250.00	86.00	1.24	2.50	20,352
13	7.57	1.71	318.90	30.00	29.99	280.00	95.00	2.70	15.10	23,001
14	7.5	3.00	451.50	45.00	24.99	465.00	75.00	1.80	10.90	31,987

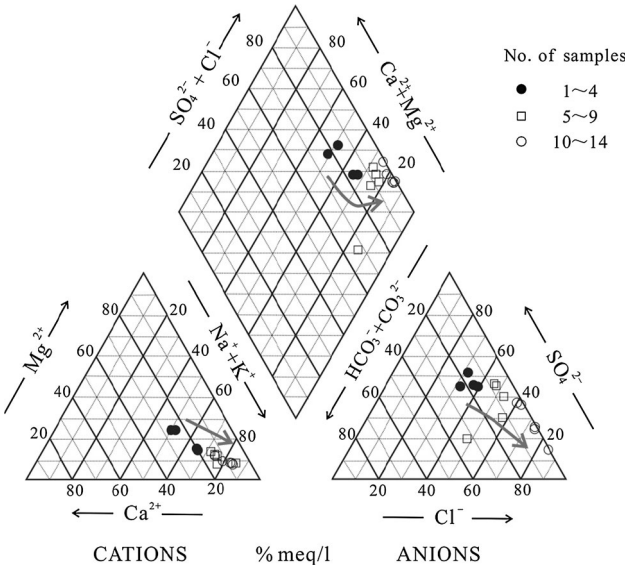

Fig. 2 Piper diagram showing proportions of major ions in groundwater from the study area

values that range between 6.77 and 7.90 with a mean value of 7.49, indicating that the groundwater is generally neutral or slightly alkaline.

Figure 2 shows the major solute concentrations plotted on a Piper trilinear diagram (Piper 1944). Among the major cations, Na^+ is dominant, comprising between 48.55 and 84.48 % of all the cations (in meq/L), whereas Ca^{2+} and Mg^{2+} range from 3.96 to 25.92 and 6.55 to 24.51 %, respectively. Among the major anions, Cl^- is dominant, comprising between 31.48 and 85.83 % of all the anions (in meq/L), whereas SO_4^{2-} and HCO_3^- range from 13.84 to 50.34 and 0.33 to 32.06 %, respectively. The groundwater displays a SO_4,Cl-Na water type in the north and a Cl,SO_4-Na water type in the south.

The TDS concentrations of the groundwater range from 1004 mg/L to 31,987 mg/L with an average value of 10,822 mg/L and generally show a trend of rising concentration from the northern mountain headwaters to the southern plains (Table 1; Fig. 1), indicating that the TDS components of the groundwater in the aquifer vary significantly and the groundwater flows from north to south. In groundwater with TDS concentrations <2000 mg/L, the relative abundance of anions is $SO_4^{2-} > Cl^- > HCO_3^-$, and in groundwater with TDS concentrations >2000 mg/L, the relative abundance of anions is $Cl^- > SO_4^{2-} > HCO_3^-$. According to the TDS values, the groundwater is slightly or moderately saline in the north but very saline or briny in the south.

Ionic relations and sources of major components in groundwater

The dissolved species and their relations with each other can reveal the origin of solutes and the process that generated the observed composition of water (Hussein 2004).

Na–Cl

The Na–Cl relationship has often been used to identify the mechanism for acquiring salinity and causing salt water intrusions in semi-arid/arid regions (Sami 1992). Na^+ and Cl^- are strongly correlated (Fig. 3) indicating that Cl^- and, for the most part, Na^+ are derived from the dissolution of halite. The slope of the fit line is 1.29, slightly greater than 1, which indicates that there is an additional source of Na^+. The ratio of Na/Cl is much greater than 1 in the northern mountainous area (Fig. 4), with a maximum value of 1.8. The high Na/Cl ratios are probably controlled by the water–rock interaction in the mountainous area, most likely

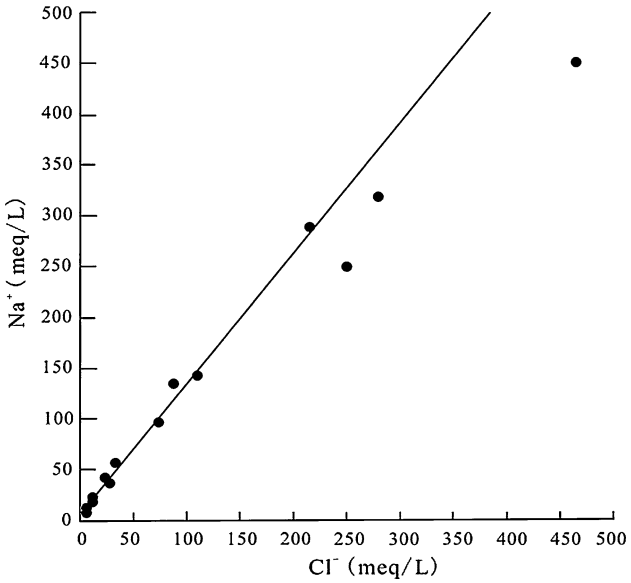

Fig. 3 Plots of Na^+ versus Cl^-

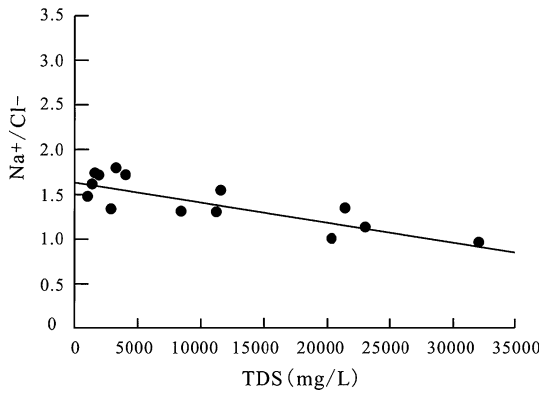

Fig. 4 Plots of Na^+/Cl^- versus TDS

by dissolution of Glauber's salt (Na_2SO_4), and feldspar weathering via reactions such as

$$Na_2SO_4 \rightarrow 2Na^+ + SO_4^{2-}$$

$$2NaAlSi_3O_8 + 2H_2O + CO_2 \rightarrow H_2Al_2Si_2O_8 + 2Na^+ + HCO_3^- + OH^-$$

Meanwhile, the ratio of Na/Cl shows a deceasing trend along the flow path of the groundwater, which is close to 1, suggesting that the dissolution of halite gradually dominates the ratio of Na/Cl, and the impact of other hydrological processes is fairly minor in the southern lacustrine plain.

Ca, Mg–HCO_3

Ca^{2+} and HCO_3^-, Mg^{2+} and HCO_3^- ($Ca^{2+} + Mg^{2+}$) and HCO_3^- show strong correlations in the samples from No. 1 to No. 9, except for No. 8 (Fig. 5). Additionally, the Mg/Ca ratios mainly vary between 0.75 and 1 (Fig. 6). These relations indicate that dolomite weathering, which is common in the limestone distributed in northern and central areas, may have an important impact on the carbonate system in the groundwater when it flows from the northern low mountains area to the middle inclined plain. The dissolved amount of gypsum is relatively little, or else the ratio of Mg/Ca would not be close to 1. However, an inverse relationship between Ca^{2+}, Mg^{2+} and HCO_3^- exists in samples No. 10 to No. 14 (Fig. 5), which may be due to the cation exchange process occurring in the groundwater when it reaches the southern alluvial lacustrine plain, leading to the rise of Ca^{2+} and Mg^{2+} concentrations and the precipitation of $CaCO_3$ and $MgCO_3$. In addition, decarbonation also contributes to the decrease in HCO_3^- because of the shallower buried depth in the southern alluvial lacustrine plain. The correlation coefficient between ($Ca^{2+} + Mg^{2+}$) and ($HCO_3^- + SO_4^{2-}$) is

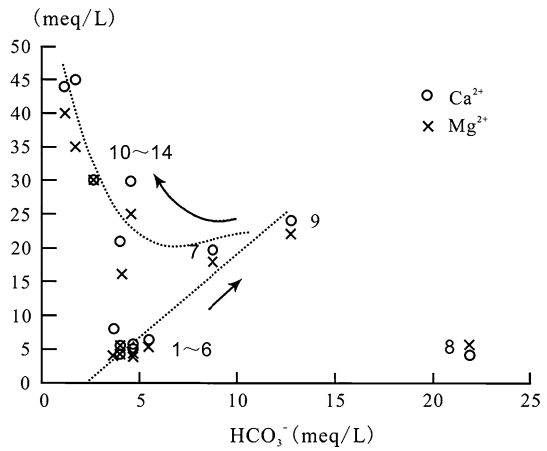

Fig. 5 Plots of Ca^{2+} and Mg^{2+} versus HCO_3^-

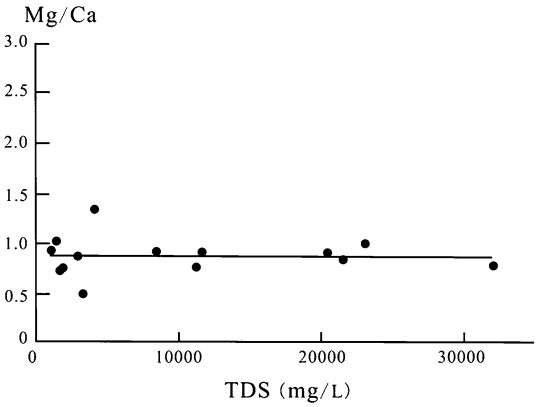

Fig. 6 Plots of Mg^{2+}/Ca^{2+} versus TDS

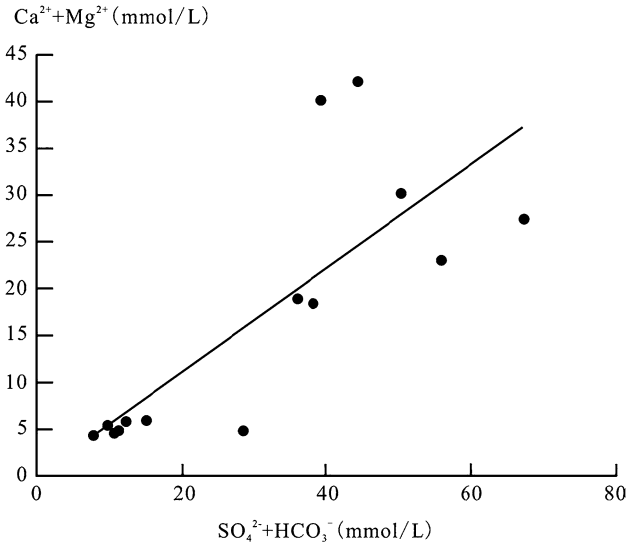

Fig. 7 Plots of ($Ca^{2+} + Mg^{2+}$) versus ($SO_4^{2-} + HCO_3^-$)

0.62, and the slope of the fit line is 0.55 (Fig. 7). If the Ca^{2+}, Mg^{2+}, HCO_3^- and SO_4^{2-} were derived from simple dissolution or precipitation of calcite, dolomite and gypsum, then a 1:1 stoichiometric ratio for ($Ca^{2+} + Mg^{2+}$) and ($HCO_3^- + SO_4^{2-}$) should exist. Therefore, an additional source of SO_4^{2-} exists, which is probably Glauber's salt, as mentioned in the Na–Cl section.

Na, Ca–SO_4

Na^+ and SO_4^{2-}, and Ca^{2+} and SO_4^{2-} show a certain degree of correlation, with correlation coefficients of 0.67 and 0.73, respectively (Figs. 8, 9). The slope of the fit line of Na^+ versus SO_4^{2-} (meq/L) is 2.92, exceeding 1, and the molar Na^+/SO_4^{2-} ratios show a rising trend along the flow path of the groundwater, with a maximum value of up to 12 (Table 2). This is probably due to the dissolution of halite with the flow of groundwater, which releases Na^+. The

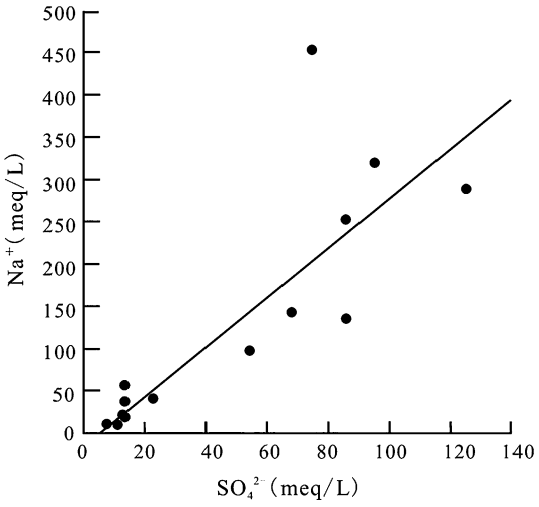

Fig. 8 Plots of Na^+ versus SO_4^{2-}

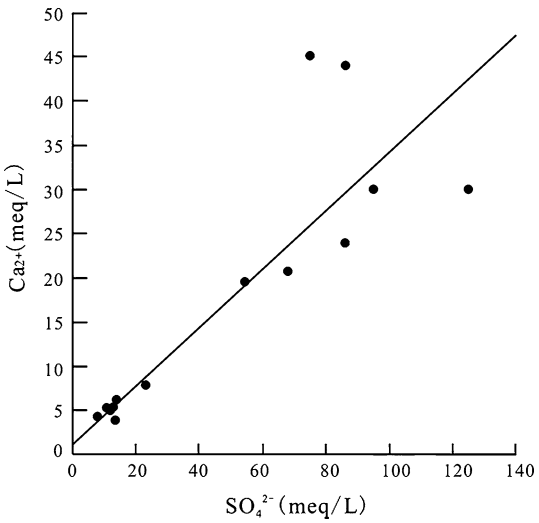

Fig. 9 Plots of Ca^{2+} versus SO_4^{2-}

slope of the fit line of Ca^{2+} versus SO_4^{2-} (meq/L) is 0.33, <1, as a result of the dissolution of Glauber's salt. Meanwhile, the molar Ca^{2+}/SO_4^{2-} ratios vary little and are mainly between 0.3 and 0.5 (Table 2), suggesting that the dissolution of Glauber's salt may only occur in the initial short flow path for groundwater, and it will not exist or will have a minor impact after the groundwater flows out of the low mountainous area.

Cation exchange

Molar Na/Ca ratios vary between 3.75 and 28.34 and increase along the groundwater flow direction (Fig. 10).

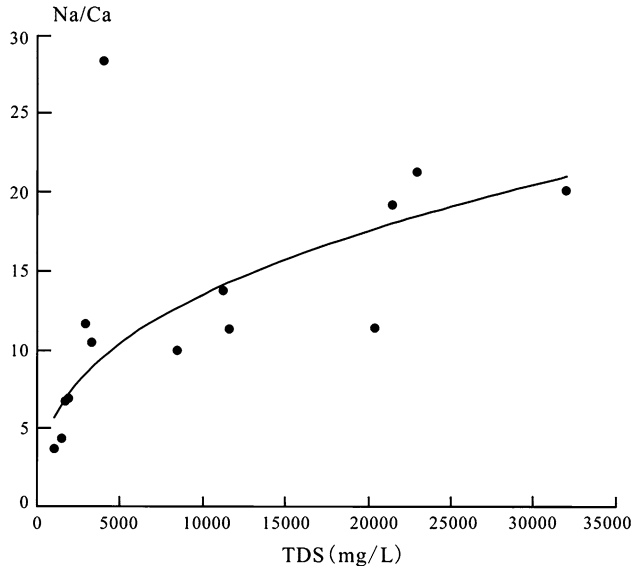

Fig. 10 Plots of Na^+/Ca^{2+} versus TDS

The existence of abundant Na^+ may promote cation exchange according to the following reaction:

$$\text{Ca-Clay(s)} + 2Na^+ \rightarrow Na_2\text{-Clay(s)} + Ca^{2+}$$

During this process, Na^+ in the solution is exchanged with Ca^{2+} in the sediments. This can be confirmed by two indices of base exchange (IBE), namely the chloro-alkaline indices (CAI 1 and CAI 2) (Schoeller 1965; Garcia et al. 2001), where

$$CAI1 = Cl - \frac{Na + K}{Cl}$$

$$CAI2 = Cl - \frac{Na + K}{SO_4} + HCO_3 + CO_3 + NO_3$$

When there is an exchange between Na^+ and K^+ in groundwater with Mg^{2+} or Ca^{2+} in the aquifer material, both of the indices are positive (Schoeller 1965). Many scholars utilized the IBE index to indicate the occurrence of cation exchange (Zhu et al. 2008; Su et al. 2009; Kumar et al. 2009; Moussa et al. 2012, 2014). In this study, all groundwater samples have positive IBE (Fig. 11), indicating that the cation exchange process occurs along the groundwater flow path.

To evaluate the effect of cation exchange, the bivariate plot of (Ca^{2+}+Mg^{2+}–SO_4^{2-}–HCO_3^-) versus (Na^+ + K^+–Cl^-) is used in which the two members vary in inverse proportions (Mc Lean et al. 2000; Garcia et al. 2001; Kamel et al. 2005; Jalali 2005, 2007; Hamed et al. 2008; Liou et al. 2009; Moussa et al. 2010). However, a few changes on the

Table 2 Mole ratios of Na to SO_4 and Ca to SO_4

Na/SO_4	2.02	2.12	2.89	2.91	3.61	5.32	3.56	8.46	3.14	4.20	4.62	5.84	6.71	12.04
Ca/SO_4	0.47	0.56	0.44	0.43	0.34	0.46	0.36	0.30	0.28	0.31	0.24	0.51	0.31	0.60

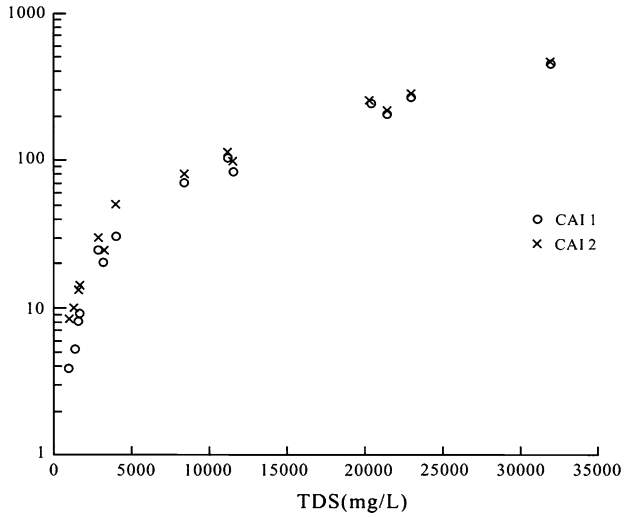

Fig. 11 Plots of (CAI 1 and CAI 2) versus TDS

axes of the diagram need to be made according to the situation in this study, where the X-axis and Y-axis should be ($Na^+ + K^+$–Cl^-–SO_4^{2-}) and ($Ca^{2+} + Mg^{2+}$–HCO_3^-) instead, respectively, because Glauber's salt is an important source of Na^+ and the dissolution of gypsum only has a minor effect on the Ca^{2+} concentration.

Therefore, the value of ($Ca^{2+} + Mg^{2+}$–HCO_3^-) represents the amount of Ca^{2+} and Mg^{2+} gained or lost from calcite and dolomite, whereas that of ($Na^+ + K^+$–Cl^-–SO_4^{2-}) is related to the amount of Na and K gained or lost from halite and Glauber's salt. If dissolution and precipitation of these minerals are the only significant processes determining the chemical composition, the data should be clustered around the original point. Furthermore, a linear relation with a slope of −1 will develop when the cation exchange between (Ca, Mg) and (Na, K) has a considerable effect on the chemical composition. In this study, the slope of the fit line is −0.97 and the correlation coefficient is 0.99 (Fig. 12), which can be further evidence of the cation exchange process.

Evaporation and precipitation

The three major mechanisms controlling world surface water chemistry can be defined as atmospheric precipitation, rock dominance, and the evaporation–crystallization process, and a Gibbs plot can be used to elucidate the major natural mechanisms controlling water chemistry (Gibbs 1970, 1971; Zhu et al. 2008; Su et al. 2009). Figure 13 shows that other dominant processes determining the water composition are evaporation and precipitation. Evaporation of surface water and moisture in the unsaturated zone has been found as the most influential process in the development of the chemical composition of shallow groundwater (Richter and Kreitler 1993). The high evaporation rate and

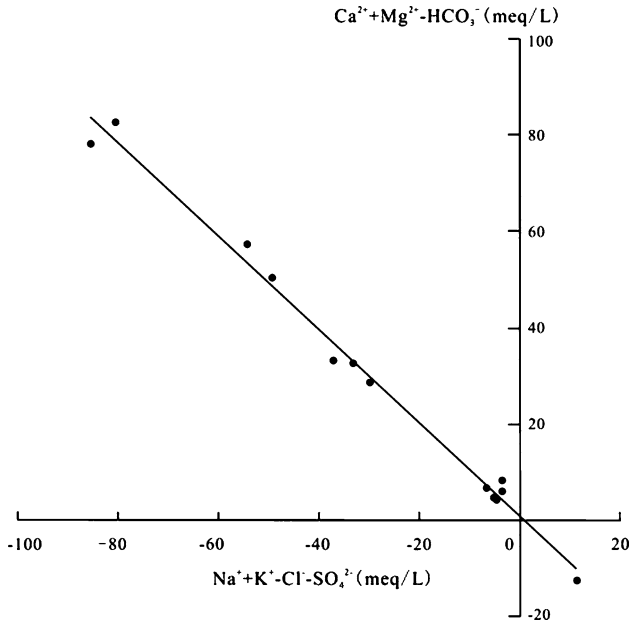

Fig. 12 Geochemical relationships showing the cation exchange process

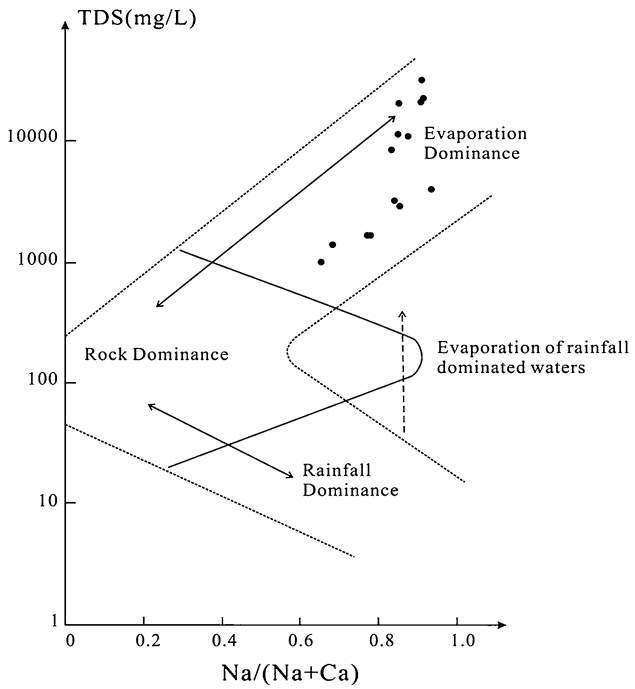

Fig. 13 A Gibbs plot indicating the mechanisms that determine the major ion composition of groundwater

low rainfall in Lop Nur promote the precipitation of low solubility evaporates.

Therefore, the major processes determining the shallow groundwater composition in the study area are dissolution of evaporates (halite, Glauber's salt, dolomite, calcite and gypsum), weathering of silicates, cation exchange, evaporation and precipitation.

Dissolution and precipitation

A mineral equilibrium calculation for groundwater was used in predicting the presence of reactive minerals in the groundwater system and estimating mineral reactivity (Deutsch 1997). By using the saturation index (SI) approach, it is possible to predict the reactive mineralogy of the subsurface from groundwater data without collecting samples of the solid phase and analyzing the mineralogy (Deutsch 1997). In this study, to determine the chemical equilibrium between minerals and water, the SI of calcite, dolomite, gypsum and halite were calculated based on the following equation (Lloyd and Heathcote 1985):

$$\mathrm{SI} = \lg \frac{\mathrm{IAP}}{K_s(T)},$$

where IAP is the ion activity product of the solution, and *Ks(T)* is the equilibrium constant of the reaction considered at temperature *T*. If the mineral is in an equilibrium state with the groundwater, the SI should be close to 0, the range of which is generally considered as 0 ± 0.5 (Deutsch 1997).

The calculated values of SI for calcite, dolomite, gypsum, and halite range from −0.5 to 1.08, −0.86 to 2.42, −1.27 to 0.02, and −6.06 to −2.61, respectively (Table 3). Figure 14 shows the SI trends for these four minerals along the flow direction of the groundwater. Halite was obviously unsaturated in the groundwater, and the value of SI rose with the groundwater flow because of the water–rock interaction and evaporation. All of the samples were below or in an equilibrium state with gypsum. The state of calcite and dolomite changed from unsaturated to oversaturated during the flowing of groundwater from the northern low mountain area to the middle inclined plain, indicating the dissolution of calcite and dolomite, which is consistent with the conclusion of ionic relations between Ca, Mg and HCO_3 in the previous section. Meanwhile, the SI values for calcite and dolomite decreased during the flowing of groundwater from the middle inclined plain to the south alluvial lacustrine plain, indicating the precipitation of these two minerals.

Table 3 Saturation index of evaporitic minerals in groundwater

No.	Calcite	Dolomite	Gypsum	Halite
1	−0.50	−0.86	−1.00	−5.82
2	−0.04	0.01	−1.17	−6.06
3	−0.03	−0.08	−0.99	−5.49
4	−0.20	−0.42	−0.97	−5.44
5	0.30	0.43	−0.72	−4.80
6	0.46	0.99	−0.98	−4.78
7	1.00	2.09	−0.27	−3.99
8	1.08	2.42	−1.27	−4.51
9	0.98	2.04	−0.10	−3.79
10	0.75	1.51	−0.22	−3.67
11	0.81	1.67	−0.01	−3.12
12	0.42	0.95	0.02	−3.11
13	0.41	0.97	−0.12	−2.96
14	0.33	0.72	−0.12	−2.61

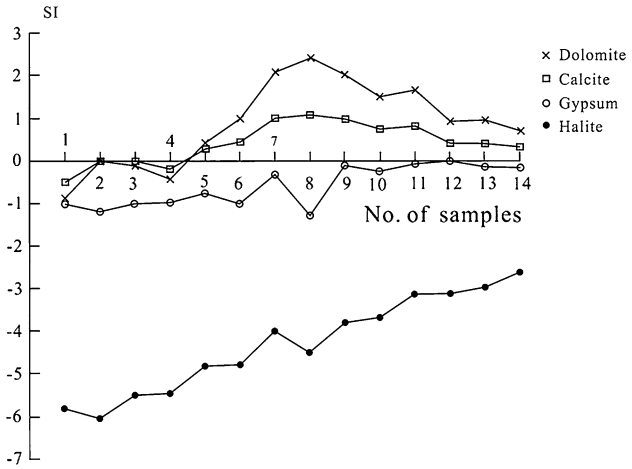

Fig. 14 Dolomite, calcite, gypsum and halite saturation index diagram of the samples from the study area

The equilibrium diagrams of gypsum, calcite and dolomite can show the trends of dissolution and precipitation controlled by the activity of corresponding ions. In the equilibrium diagrams of gypsum (Fig. 15), $\mathrm{pCa}^{2+} = \lg r_{\mathrm{Ca}}^{2+}$, $\mathrm{pSO_4}^{2-} = -\lg r_{\mathrm{SO4}}^{2-}$, $\mathrm{p}K_{\mathrm{gyp}} = \lg(r_{\mathrm{Ca}}^{2+} \cdot r_{\mathrm{SO4}}^{2-}) = \mathrm{pCa}^{2+} + \mathrm{pSO_4}^{2-}$, where r is the ion activity, and K_{gyp} is the equilibrium constant of gypsum. Therefore, the line $\mathrm{p}K_{\mathrm{gyp}} = \mathrm{pCa}^{2+} + \mathrm{pSO_4}^{2-} = -4.6$ at 25 °C is the equilibrium line of gypsum (Morel and Hering 1993; Stumm and Morgan 1981; Matthess 1982), and the samples under (above) the line are unsaturated (oversaturated). When the data points are distributed along the dotted line 1, it indicates the existence of a source of $\mathrm{SO_4}^{2-}$ and the lack of a source of Ca^{2+} in the aquifer. Additionally, if the data points cross the line $\mathrm{p}K_{\mathrm{gyp}}$, gypsum will precipitate; meanwhile, if the source of $\mathrm{SO_4}^{2-}$ continuously provides $\mathrm{SO_4}^{2-}$ for the groundwater, the Ca^{2+} content will decrease because of the precipitation of gypsum, similar to the trend of the dotted line 4 in Fig. 15. Similarly, dotted line 2 and line 5 show other extreme cases. In most cases, the minerals in the aquifer can release Ca^{2+} and $\mathrm{SO_4}^{2-}$ simultaneously, as shown by the trend of line 3. The samples in this study evolve along line 3 and then along line 5 (Fig. 15), which demonstrates that there are sources of Ca^{2+} and $\mathrm{SO_4}^{2-}$ in the aquifer and that gypsum finally reaches equilibrium with groundwater. Then the content of Ca^{2+} increases continuously, leading to the decrease in $\mathrm{SO_4}^{2-}$. The reason for the increase in Ca^{2+} is probably the cation exchange process, as demonstrated by the previous analysis in this study.

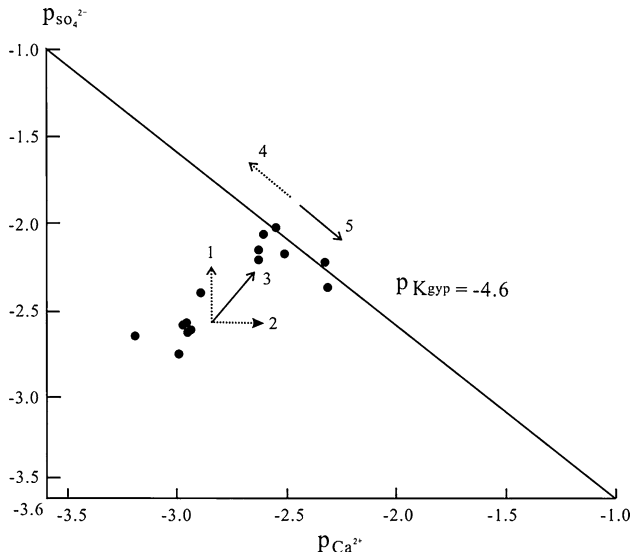

Fig. 15 SO_4^{2-} and Ca^{2+} activity and equilibrium of gypsum

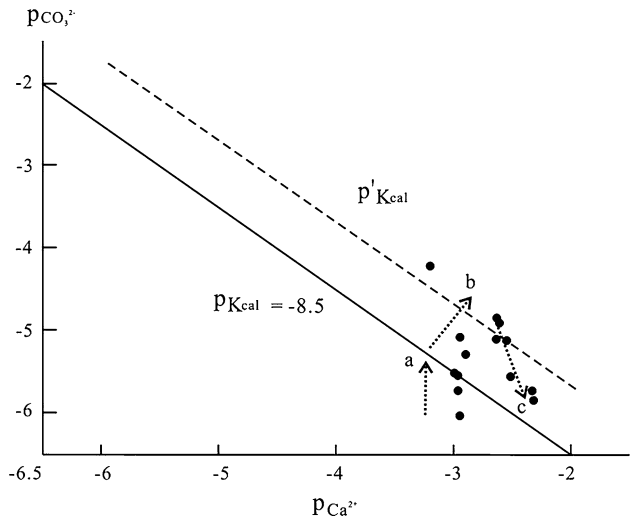

Fig. 16 CO_3^{-} and Ca^{2+} activity and equilibrium of calcite

The principal equilibrium diagrams of calcite and dolomite (Figs. 16, 17) are similar to gypsum. In Figs. 16 and 17, the dotted lines (a) (b), and (c) show the trends of the distribution of data points. Dotted line (a) is likely the result of dissolution of CO_2. Dotted line (b) indicates the dissolution of calcite and dolomite, and some of data points exceed the line pK_{cal} (Fig. 16) and pK_{dol} (Fig. 17) up to dotted line $p'K_{cal}$ and $p'K_{dol}$, which demonstrates the increasing of solubility of these two minerals in groundwater under some special environmental conditions. According to the status of groundwater in this area, the reasons for this phenomenon are probably the salt effect and high CO_2 partial pressure in the groundwater because the high concentration of chloride and sulfate in the groundwater could

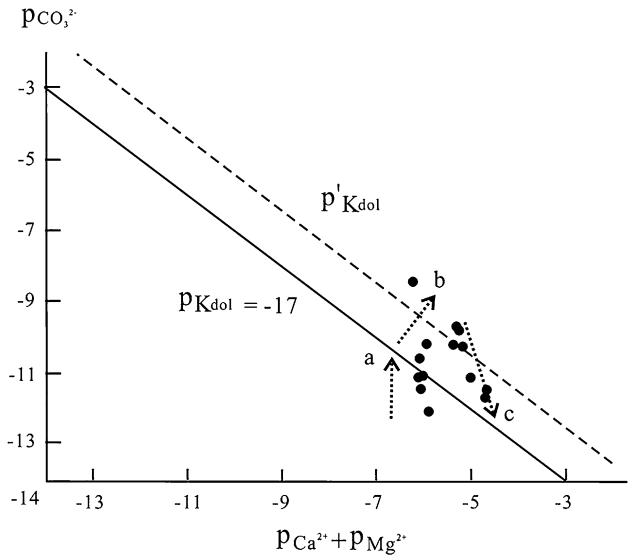

Fig. 17 CO_3^{-}, Ca^{2+} and Mg^{2+} activity and equilibrium of dolomite

increase the solubility of calcite and dolomite due to the salt effect (Yan 2008, 2009; Busenber and Plummer 1985), and high CO_2 partial pressure could promote the dissolution of calcite and dolomite (Morse and Arvidson 2002; Pokrosky et al. 2005, Yan et al. 2009). Dotted line (c) indicates the precipitation of calcite and dolomite.

Inverse geochemical modeling

Combining the above geochemical analyses, inverse geochemical modeling can be utilized to quantitatively simulate the hydrochemical evolution of groundwater. The simulation can be divided into two paths according to the flow path of the groundwater. The first path is to simulate the first process, i.e., groundwater flow from the northern mountainous area to the middle inclined plain, by assuming that groundwater flows from sample 1 to sample 9. The second path is to simulate the rest of the flow path of groundwater, which is from the middle inclined plain to the southern alluvial lacustrine plain, by assuming that groundwater flows from sample 9 to sample 14. The elements involved in these modeled phases include the following: Ca, Mg, Na, K, S, Cl, Si, C and Al, which are all constrained by mass balance. In this study, PHREEQC 2.14.2 is employed to model the two paths.

Path 1

Because the solutions of inverse geochemical modeling are always multiple, some reasonable constraint conditions should be set based on the previous geochemical analysis:

1. Evaporitic minerals, including halite and Glauber's salt, are highly soluble and are forced to dissolve in the

Table 4 The mass transfers of 6 possible models obtained from inverse geochemical simulation in path 1 (mmol/L)

No.	Halite	Dolomite	Calcite	Glauber's salt	Albite	K-feldspar	Na^+	Ca^{2+}	Mg^{2+}	Illite	SiO_2	CO_2
Model 1	80.68	1.97	–	37.88	–	1.97	−28.36	7.517	6.66	−0.86	−2.84	4.12
Model 2	80.68	8.63	−13.32	37.88	–	1.97	−28.36	14.18	–	−0.86	−2.84	4.12
Model 3	35.45	–	−21.99	–	62.29	21.99	−62.29	21.99	916	−36.64	−1.25	21.98
Model 4	80.68	–	3.93	37.88	–	1.97	−28.36	5.55	8.63	−0.86	−2.84	4.12
Model 5	35.45	916.0	−40.31	–	62.29	21.99	−62.29	31.15	–	−36.64	−1.25	21.98
Model 6	80.68	–	–	37.88	11.13	5.90	−39.49	9.48	10.26	−7.41	−25.11	8.05

– no mass transfer

A positive (negative) value indicates entering (exiting) of the groundwater system

Table 5 The mass transfers of 11 possible models obtained from inverse geochemical simulation in path 2

No.	Halite	Gypsum	Dolomite	Calcite	Albite	K-feldspar	Na^+	Ca^{2+}	Mg^{2+}	Illite	SiO_2	CO_2
Model 1	373.3	–5.55	−2.79	–	<0.01	–	−56.64	18.96	9.36	–	−0.07	−5.98
Model 2	373.3	–5.56	−5.77	–	16.94	5.98	−73.59	21.96	14.84	−9.96	−33.95	–
Model 3	373.3	−5.55	–	−5.57	<0.01	–	−56.64	21.75	6.57	–	−0.07	−5.98
Model 4	373.3	−5.56	–	−11.55	16.94	5.98	−73.59	27.73	9.06	−9.96	−33.95	–
Model 5	373.3	−5.55	6.57	−18.71	<0.01	–	−56.64	28.32	–	–	−0.07	−5.98
Model 6	373.3	−5.55	−21.75	37.93	<0.01	–	–56.64	–	28.32	–	−0.07	−5.98
Model 7	373.3	−5.56	9.06	−29.67	16.94	5.98	−73.59	36.79	–	−9.96	−33.95	–
Model 8	373.3	−5.56	−27.73	43.92	16.94	5.98	−73.59	–	36.79	−9.96	−33.95	–
Model 9	–	−181.5	−694.0	–	39.32	13.88	−39.34	695.4	12.72	−23.13	−78.63	13.87
Model 10	–	−181.5	577.8	−25.44	39.32	13.88	−39.34	19.67	–	−23.13	−78.63	13.87
Model 11	–	−181.5	−13.89	13.91	39.32	13.88	−39.34	–	19.67	−23.13	−78.63	13.87

– no mass transfer

A positive (negative) value indicates entering (exiting) of the groundwater system

model according to the analysis results of ionic relations and SI trends for these two minerals. Dolomite and calcite are allowed to dissolve and precipitate.

2. Silicate minerals, including albite and K-feldspar, are common in the northern mountainous area and are forced to dissolve. Quartz (or aqueous silica) is a potential product in the alteration of albite and K-feldspar; therefore, both dissolution and precipitation processes are allowed for SiO_2.
3. Illite is a common weathering product and is distributed in the aquifer in the middle and south of the study area according to the borehole data; therefore, it is forced to precipitate in the model.
4. CO_2 is a very common phase in geochemical reactions of the groundwater system and can enter and exit the groundwater system in the model.
5. Cation exchange is set to occur in the model based on the previous analysis on cation exchange.

The simulation obtains 6 possible models, as shown in Table 4. According to the analysis results of geochemical interpretations, dolomite dissolution is one of the dominant processes for geochemical evolution of groundwater. Therefore, Model 3, Model 4 and Model 6 can be excluded. Meanwhile, the dissolution amount of albite and K-feldspar is large in Model 5, which is less plausible because they are insoluble minerals. Finally, Model 1 and Model 2 are more plausible than the others. The difference between Model 1 and Model 2 is whether incongruent dissolution of dolomite occurs, which is dolomite dissolution with calcite precipitation, and it cannot be determined.

According to the simulation results, the conceptual model of the geochemical reactions governing the mass transfer of water–rock interaction can be described by

$$\begin{aligned}&\text{Sample 1} + \text{Halite} + \text{Glauber's salt} + \text{Dolomite}\\&\quad + \text{K-feldspar} + \text{Ca}^{2+}\left(\text{Mg}^{2+}\right) + \text{CO}_2\\&\quad \rightarrow \text{Sample 9} + \text{Na}^+ + \text{SiO}_2 + \text{Illite} + (\text{Calcite})\end{aligned}$$

Path 2

The constraint conditions in path 2 are approximately the same as in path 1, except for Glauber's salt and gypsum.

Firstly, because there is no Glauber's salt in the central and southern areas, it should be excluded from the reactants. Secondly, gypsum has reached equilibrium in the beginning of path 2, and it probably precipitates from groundwater in path 2 because of cation exchange, leading to the increase in Ca^{2+}; therefore, gypsum is forced to precipitate in the simulation for path 2.

The simulation obtains 11 possible models, as shown in Table 5. Obviously, the dissolution of albite is too large in Model 2, Model 4, Model 7, Model 8, Model 9, Model 10 and Model 11, which is less possible because it is an insoluble mineral. Model 1, Model 3, Model 5 and Model 6 are more plausible than the others. The differences between them are whether the carbonate precipitating from groundwater is calcite or dolomite and whether incongruent dissolution of dolomite and calcite occurs.

According to the simulation results, the conceptual model of the geochemical reactions governing the mass transfer of the water–rock interaction can be described by

$$\begin{aligned}&\text{Sample 9} + \text{Halite} + \text{Albite} + Ca^{2+}\left(Mg^{2+}\right)\\ &\rightarrow \text{Sample 14} + \text{Gypsum} + \text{Dolomite(Calcite)} + Na^{+}\\ &\quad + SiO_2 + \text{Illite} + CO_2\end{aligned}$$

The simulation results for two paths are consistent with analyses in previous sections of this study.

Conclusions

Based on the concept of water–rock interaction, hydrochemical characteristics and geochemical modeling are effective ways to understand the geochemical evolution of groundwater. The main conclusions are as follows:

The trends in major ions in the groundwater of the study area show the geochemical evolution process of groundwater. Overall, the shallow groundwater in the northern low mountains area is SO_4,Cl-Na type with low TDS, <2000 mg/L, changing to Cl,SO_4-Na type with high TDS along the groundwater flow direction, with TDS reaching up to 31,987 mg/L, which demonstrates that the shallow groundwater is recharged in the north and discharged in the south. From the ionic relation plots, the water–rock reaction and evaporation are dominated factors that determine the major ionic composition in the study area. In addition to the dissolution of halite, the high ratio of Na^+/Cl^- in the northern area indicates a significant contribution of Na^+ from Glauber's salt (Na_2SO_4) and silicate weathering (Albite and K-feldspar). Glauber's salt is also responsible for SO_4^{2-}. The samples collected from the northern and central areas show strong correlations between (Ca^{2+} + -Mg^{2+}) and HCO_3^-, and the ratio of Mg/Ca is close to 1, which indicates that dissolution of dolomite is probably involved. The high ratio of Na^+/Ca^{2+} may promote cation exchange, which can supply Ca^{2+} or Mg^{2+}, and could lead to the precipitation of calcite or dolomite. Therefore, cation exchange has an impact on the status of carbonate in groundwater and is likely the reason for the inverse relationship between Ca^{2+}, Mg^{2+} and HCO_3^- existing in the samples collected from the southern area.

The SI of halite, gypsum, calcite and dolomite show that halite is unsaturated and dissolves in groundwater throughout the entire process; gypsum gradually becomes saturated with the flowing of groundwater, and calcite and dolomite dissolve in the groundwater when the groundwater flows from the northern area to the middle area and then precipitate from the groundwater during the remaining flow path. The equilibrium diagrams of these minerals also reveal these processes.

PHREEQC is used to simulate the predominant geochemical reactions controlling the chemical evolution of the groundwater. The results demonstrate that halite and Glauber's salt are major sources of Na^+, Cl^- and SO_4^{2-}. Cation exchange adds a certain amount of Ca^{2+} and Mg^{2+}, which impacts the equilibrium state of calcite and dolomite with groundwater.

Based on the above evidence, it can be concluded that the shallow groundwater in northwest margin of Lop Nur was characterized by high salinity and slow circulation. The dissolution of halite, Glauber's salt, dolomite and calcite determined the Na^+, Cl^-, Mg^{2+}, Ca^{2+}, SO_4^{2-} and HCO_3^- chemistry, but evaporation and precipitation also influenced the water composition. The groundwater in the northern low mountains has strong corrosion capacity to carbonatite, thus changing the carbonate composition in the south area, which promotes the diagenesis of carbonatite in this area as well.

Acknowledgments This research was supported by National Natural Science Foundation of China (Grant No. 41030746, 41172207 and 41102147).

Compliance with ethical standards

Conflict of interest The authors declare that they have no conflict of interest.

References

Al-Charideh A (2012) Geochemical and isotopic characterization of groundwater from shallow and deep limestone aquifers system of Aleppo basin (north Syria). Environ Earth Sci 65(4):1157–1168

Busenber GE, Plummer LN (1985) Kinetic and thermodynamic factors controlling the distribution of SO_4^{2-} and Na^+ in calcite and selected aragonites. Geochemica et Cosmochimica Acta 49(2):713–725

Chang H, An ZS, Liu WG, Qiang XK, Song YG, Ao H (2012) Magnetostratigraphic and paleoenvironmental records for a Late Cenozoic sedimentary sequence drilled from Lop Nor in the eastern Tarim Basin. Global Planet Change 80–81(1):113–122

Demiroglu M, Orgun Y, Yaltirak C (2011) Hydrogeology and hydrogeochemistry of Gunyuzu semi-arid basin (Eskisehir, Central Anatolia). Environ Earth Sci 64(5):1433–1443

Deutsch WJ (1997) Groundwater geochemistry: fundamentals and application to contamination. CRC Press, Boca Raton

Dong ZB, Lv P, Qian GQ, Xia XC, Zhao YJ, Mu GJ (2012) Research progress in China's Lop Nur. Earth Sci Rev 111(1):142–153

Duan HM, Kurban A, Zhang Y, Ablekim A (2013) Review of the studies about the latest dried-up time of the Lop Nur lake in recent 100 years. Arid Zone Research 30(3):541–549

Edmunds M (2003) Renewable and non-renewable groundwater in semi-arid and arid regions. In: Alsharhan AS, Wood WW (eds) Water resources perspectives: evaluation. Management and policy. Elsevier, Amsterdam, pp 1–15

Garcia MG, Hidalgo MDV, Blesa MA (2001) Geochemistry of groundwater in the alluvial plain of Tucuman province, Argentina. Hydrogeol J 9(6):597–610

Gibbs R (1970) Mechanism controlling world river water chemistry. Science 170:1088–1090

Gibbs R (1971) Mechanism controlling world river water chemistry: evaporation–crystallization process. Science 172:871–872

Han DM, Song XF, Currell MJ, Cao GL, Zhang YH, Kang YH (2011) A survey of groundwater levels and hydrogeochemistry in irrigated fields in the Karamay agricultural development area, northwest China: implications for soil and groundwater salinity resulting from surface water transfer for irrigation. J Hydrol 405(3):217–234

Hussein MT (2004) Hydrochemical evaluation of groundwater in the Blue Nile Basin, eastern Sudan, using conventional and multivariate techniques. Hydrogeol J 12(2):144–158

Jalali M (2005) Major ion chemistry of groundwaters in the Bahar area, Hamadan, western Iran. Environ Geol 47(6):763–772

Jalali M (2007) Assessment of the chemical components of Famenin groundwater, western Iran. Environ Geochem Health 29(5):357–374

Jiao PC, Liu CL, Qi JX, Wang ML, Chen YZ (2003a) Collection of samples from underground high-salinity brine for ^{14}C dating. Earth Sci Front 10(1):309–312 **(in Chinese with English abstract)**

Jiao PC, Liu CL, Wang ML, Chen YZ, Wang XM (2003b) Characteristics and dynamic analysis of inter-crystal brine movement in the Lop Nur salt lake. Acta Geoscientia Sinica 24(3):255–260 **(in Chinese with English abstract)**

Jiao PC, Wang ML, Liu CL (2004) Characteristics and origin of tritium in the potassium rich brine in Lop Nur, Xinjiang. Nucl Tech 27(9):710–715 **(in Chinese with English abstract)**

Jiao PC, Liu CL, Bai DM, Wang ML, Chen YZ (2005) Application of self-potential technique to the exploration of potassium-rich brine in Lop Nur, Xinjiang. Acta Geoscientia Sinica 26(4):381–385 **(in Chinese with English abstract)**

Kamel S, Dassi L, Zouari K, Abidi B (2005) Geochemical and isotopic investigation of the aquifer system in the Djerid-Nefzaoua basin, southern Tunisia. Environ Geol 49(1):159–170

Kumar M, Kumari K, Singh UK, Ramanathan AL (2009) Hydrogeochemical processes in the groundwater environment of Muktsar, Punjab: conventional graphical and multivariate statistical approach. Environ Geol 57(4):873–884

Li BG, Ma LC, Jiang PA, Duan ZQ, Sun DF, Qiu HL, Zhong JP et al (2008) High precision topographic data on Lop Nor basin's lake "Great Ear" and the timing of its becoming a dry salt lake. Chin Sci Bull 53(6):905–914

Liou TS, Lu HY, Lin CK, Lin W, Chang YT, Chien JM, Chen WF (2009) Geochemical investigation of groundwater in a Granitic Island: a case study from Kinmen Island, Taiwan. Environ Geol 58(7):1575–1585

Liu CL, Wang ML, Jiao PC (1999) Hydrogen, oxygen, strontium and sulfur isotopic geochemistry and potash-forming material sources of Lop salt lake, Xinjiang. Miner Dep 18(3):268–275 **(in Chinese with English abstract)**

Liu CL, Wang ML, Jiao PC, Chen YZ (2002) Formation of pores and brine reversing mechanism of the aquifers in Quaternary potash deposits in Lop Nur lake, Xinjiang, China. Geol Rev 48(4):437–444 **(in Chinese with English abstract)**

Liu CL, Jiao PC, Wang ML, Li SD, Chen YZ (2003a) Ascending brine fluids in Quaternary salty lake of Lop Nur in Xinjiang and their significance in potash formation. Miner Depos 22(4):386–392 **(in Chinese with English abstract)**

Liu CL, Jiao PC, Wang ML, Yang ZC, Li SD, Chen YZ (2003b) Characteristics of diagenesis of the Quaternary salt-bearing strata, Lop Nur lake, Xinjiang. Acta Sedimentol Sin 21(2):240–246 **(in Chinese with English abstract)**

Liu CL, Wang ML, Jiao PC, Chen YZ (2009) The probing of regularity and controlling factors of potash deposits distribution in Lop Nur Salt Lake. Acta Geosci Sin 30(6):796–802 **(in Chinese with English abstract)**

Liu CL, Ma LC, Jiao PC, Sun XH, Chen YZ (2010) Chemical sedimentary sequence of Lop Nur salt lake in Xinjiang and its controlling factors. Miner Depos 29(4):625–630 **(In Chinese with English abstract)**

Lloyd JW, Heathcote JA (1985) Natural inorganic hydrochemistry in relation to groundwater. Oxford University Press, New York

Luo C, Peng ZC, Liu WG, Zhang ZF, He JF, Liu GJ, Zhang PX (2008a) Evidence from the lacustrine sediments of Lop Nur Lake, northwest China for the Younger Dryas event. Earth Sci J China Univ Geosci 33(2):190–196 **(In Chinese with English abstract)**

Luo C, Peng ZC, Yang D, Liu WG, He JF (2008b) Paleoclimate of Lop Nur and the response to global change by geochemical elements multi-analysis. Geochemica 37(2):139–148 **(In Chinese with English abstract)**

Ma LC, Lowenstein TK, Li BG, Jiang PG, Liu CL, Zhong JP, Sheng JD et al (2010) Hydrochemical characteristics and brine evolution paths of Lop Nor Basin, Xinjiang Province, Western China. Appl Geochem 25(11):1770–1782

Matthess G (1982) The properties of groundwater. Wiley, New York, p 406

McLean W, Jankowski J, Lavitt N (2000) Groundwater quality and sustainability in alluvial aquifer, Australia. In: Sielilo et al (eds) Groundwater, past achievement and future challenges. Bolkema, Rotterdamm, pp 567–573

Morel FMM, Hering JG (1993) Principles and applications of aquatic chemistry. Wiley, New York, p 588

Morse JW, Arvidson RS (2002) The dissolution kinetics of major sedimentary carbonate minerals. Earth Sci Rev 58(1):51–84

Moussa AB, Salem SBH, Zouari K, Jlassi F (2010) Hydrochemical and isotopic investigation of the groundwater composition of an alluvial aquifer, Cap Bon Peninsula, Tunisia. Carbonates Evaporites 25(3):161–176

Moussa AB, Zouari K, Valles V, Jlassi F (2012) Hydrogeochemical analysis of groundwater pollution in an irrigated land in Cap Bon Peninsula, North-Eastern Tunisia. Arid Land Res Manag 26(1):1–14

Moussa AB, Mzali H, Zouari K, Hezzi H (2014) Hydrochemical and isotopic assessment of groundwater quality in the Quaternary shallow aquifer, Tazoghrane region, north-eastern Tunisia. Quatern Int 338(4):51–58

Parkhurst DL, Appelo CAJ (1999) User's Guide to PHREEQC (version 2): a computer program for speciation, batch-reaction, one dimensional transport, and inverse geochemical calculations, water-resources investigations Report. US Geological Survey, Reston, pp 99–4259

Piper AM (1944) A graphic procedure in the geochemical interpretation of water-analyses. Trans Am Geophys Union 25(6):914–928

Pokrosky OS, Golubev SV, Schott J (2005) Dissolution kinetics of calcite, dolomite and magnesite at 25°C and 0 to 50 atm pCO_2. Chem Geol 217(3–4):239–255

Richter BC, Kreitler WC (1993) Geochemical techniques for identifying sources of groundwater salinization. CRC Press, New York, pp 14–26

Rouabhia A, Baali F, Fehdi C, Abderrahmane B, Djamel B (2011) Hydrogeochemistry of groundwaters in a semi-arid region. El Ma El Abiod aquifer, Eastern Algeria. Arab J Geosci 4(5):973–982

Sami K (1992) Recharge mechanisms and geochemical process in a semi-arid sedimentary basin, Eastern cape, South African. J Hydrol 139(1–4):27–48

Schoeller H (1965) Qualitative evaluation of groundwater resources. In: Methods and techniques of groundwater investigations and development. UNESCO, Paris, pp 4–83

Song SM (2009) Lop Nur area's environmental variation during the different historical periods. Arid Land Geogr 32(1):107–111 **(in Chinese with English abstract)**

Stumm W, Morgan JJ (1981) Aquatic chemistry, 2nd edn. Wiley, New York, p 780

Su YH, Zhu GF, Feng Q, Li ZZ, Zhang FP (2009) Environmental isotopic and hydrochemical study of groundwater in the Ejina Basin, northwest China. Environ Geol 58(3):601–614

Wang ML, Liu CL, Jiao PC (2001) Saline lake potash resources in the Lop Nur. Geological Press, Beijing **(in Chinese with English summary)**

Wang FB, Ma CM, Xia XC, Cao QY, Zhu Q (2008) Environmental evolution in Lop Nur since the late Pleistocene and its response to the global changes. Quat Sci 28(1):150–153 **(in Chinese with English abstract)**

Xia XC, Wang FB, Zhao YJ (2007) Lop Nur in China. Science Press, Beijing **(In Chinese)**

Xiao XC, He GQ, Xu X (2010) Crustal tectonic framework and geological evolution of Xinjiang uygur autonomous region of China. Geological Publishing House, Beijing **(in Chinese)**

Yan ZW (2008) Influences of SO_4^{2-} on the solubility of calcite and dolomite. Carsologica Sin 27(1):24–31 **(in Chinese with English abstract)**

Yan ZW, Zhang ZW (2009) The effect of chlorite on the solubility of calcite and dolomite. Hydrogeol Eng Geol 36(1):113–118 **(in Chinese with English abstract)**

Yan S, Mu GJ, Xu YQ (1998) Quaternary environmental evolution of the Lop Nur region, China. Acta Geogr Sin 53(4):332–340 **(in Chinese with English abstract)**

Yan ZW, Liu HL, Zhang ZW (2009) Influences of temperature and P_{CO2} on the solubility of calcite and dolomite. Carsologica Sin 28(1):7–10 **(In Chinese with English abstract)**

Yang D, Peng ZC, Luo C, Liu Y, Zhang ZF, Liu WG, Zhang PX (2013) High-resolution pollen sequence from Lop Nur, Xinjiang, China: implications on environmental changes during the late Pleistocene to the early Holocene. Rev Palaeobot Palynol 192:32–41

Zhao YJ, Xia XC, Wang FB, Cao QY, Gao WM, You GY (2006) Features and causes of formation on ring-shaped salt crust in Lop Nur region of Xinjiang, China. Arid Land Geogr 29(6):779–783 **(in Chinese with English abstract)**

Zhao HT, Liu CL, Jiao PC, Sun XH, Li DX (2014) Morphology characteristics and influential factors of glauberite growth from Lop Nur Salt Lake, China. Acta Mineral Sin 34(1):97–106 **(in Chinese with English abstract)**

Zhong JP, Qiu HL, Dong XG, Jiang PA, Wu HQ, Yang PN (2005) Discussion on the dried-up time of the Lop Nur Lake. Arid Land Geogr 28(1):6–9 **(in Chinese with English abstract)**

Zhong JP, Ma LC, Li BG, Jiang PA, Qiu HL, Wu HQ (2008) Rediscussion on the latest drying up of the "Great Ear" in the Lop Nor area. Arid Land Geogr 31(1):101–116 **(in Chinese with English abstract)**

Zhu GF, Su YH, Feng Q (2008) The hydrochemical characteristics and evolution of groundwater and surface water in the Heihe River Basin, northwest China. Hydrogeol J 16(1):167–182

Zhu Q, Wang FB, Cao QY, Xia XC, Li SF, Ma CM (2009) Grain size distribution characteristics and changes of Lop Nur Lake during the past 10,000 years. J Stratigr 33(3):283–290 **(in Chinese with English abstract)**

Zhu BQ, Yang XP, Rioual P, Qin XG, Liu ZT, Xiong HG, Yu JJ (2011) Hydrogeochemistry of three watersheds (the Erlqis, Zhungarer and Yili) in northern Xinjiang, NW China. Appl Geochem 26(8):1535–1548